Quantum Electronics **40** (2) 149 – 152 (2010)

RADIATION SCATTERING

PACS numbers: 52.38.–r; 42.25.Fx
DOI: 10.1070/QE2010v040n02ABEH014150

Peculiarities of the angular distribution of laser radiation intensity scattered by laser-spark plasma in air

A.A. Malyutin, V.A. Podvyaznikov, V.K. Chevokin

***Abstract*. The spatiotemporal study of the diagram of laser radiation scattering by the laser-spark plasma produced by 3-ns and 50-ns pulses is performed. It is shown that radiation appearing outside the laser beam cone is scattered during the first one – two nanoseconds after the air breakdown, when the spark plasma is located in the vicinity of the laser beam waist and has a shape close to spherical.**

Keywords: *laser spark, laser radiation scattering by the spark plasma.*

1. Introduction

The prediction [1] and subsequently repeated experimental confirmation of the possibility of laser radiation self-focusing in optical media [2 – 4] and the discovery of the air breakdown (laser spark) by laser radiation [5] have come about during a short period of time. It is not surprising, then, that in the case of a laser spark, these two phenomena, requiring high-power laser pulses, were considered by some researches as following one from another. It was not clear only whether the spark plasma formation precedes self-focusing or vice versa. Once it has been found out that the nonlinearity of gases under normal conditions is too small for self-focusing to appear [6], several possible mechanisms of radiation self-focusing in plasma were proposed. However, the validity of these mechanisms in a laser spark initiated by nanosecond pulses in gases was not experimentally confirmed so far. The case of femtosecond pulses is a special one, and we do not consider it here.

For a long time it was accepted that the main manifestations of self-focusing during optical breakdown in gases were the presence of a narrow scattering channel observed from the side (the so-called plasma filaments) and forward scattering of radiation outside the beam cone accompanying a laser spark [7]. The first phenomenon, as shown in our previous work [8], is not related to self-focusing and is inherent in the reflection of laser radiation from the plasma-unperturbed gas interface. It was also shown earlier [9] that the angular dependence of the forward scattering intensity could be calculated as the diffraction of radiation from a laser spark plasma. However, radiation scattering by the spark plasma was not studied, although it was clear that the measurement of the time dependence of the intensity of this radiation could clarify the mechanism of its formation.

In principle, such experiments were already reported in earlier papers [10, 11], where only the steep front of a scattering pulse was observed. Later on, measurements were performed with the time resolution providing the recording of quite short pulses with the front duration down to ~ 100 ps in the radiation propagated through a laser spark (i.e. within the laser beam cone) and in its component scattered at large angles [12]. In the cone of scattered laser radiation behind the laser spark, pulses with the amplitude noticeably exceeding the laser pulse amplitude in the absence of the spark were also observed [13], as well as an interference pattern [14]. These experimental data were treated as reflection from the spark plasma boundary [12] or laser radiation self-focusing [13, 14].

Experiments described in the present paper pursued two goals. First, we investigated in detail the spatiotemporal diagram of laser radiation scattering by the spark plasma and, second, attempted to find the specific features in the spark dynamics in the beam-waist vicinity, if they exist. The latter mainly concerns scattering at an angle of 90° to the laser beam direction. This part of the scattering diagram is of interest because laser radiation scattering, as pointed out in [8], is the most intense outside the laser-beam waist, whereas in the waist region [$\pm(20-25)$ μm from the focal plane of a lens] it is weak and cannot be detected in fact upon integrated recording per pulse.

2. Experiment

We used a neodymium GLS 23 glass laser and a Nd : YAG laser in experiments. The first laser emitted 50 ± 5-ns, 50-mJ pulses and could operate in the single-frequency regime at the TEM_{00} and TEM_{01} modes [15]. The second laser emitted 3.2 ± 0.1-ns, 4-mJ pulses (the resonator length was 25 cm, and a 1055 dye in a plastic matrix with transmission of 18 % was used as a Q switch). This laser also emitted single-frequency radiation at the TEM_{00} mode.

Laser radiation was focused in the laboratory air at the normal pressure by aspherical lenses [16] with focal distances $f = 8$ and 20 mm. In the latter case, the numerical aperture of a focused laser beam was increased (for both lenses, NA = 0.5) by mounting a $3^{\times}$ Galilean telescope in front of a lens so that the condition $2w/f \approx 0.4$ was fulfilled

A.A. Malyutin, V.A. Podvyaznikov, V.K. Chevokin A.M. Prokhorov General Physics Institute, Russian Academy of Sciences, ul. Vavilova 38, 119991 Moscow, Russia; e-mail: amal@kapella.gpi.ru

Received 7 May 2009; revision received 28 September 2009
Kvantovaya Elektronika **40** (2) 149 – 152 (2010)
Translated by M.N. Sapozhnikov

for both lenses (w is the beam radius on the lens) and the calculated waist diameter $2w_f$ was 4 μm.

The diagram of laser radiation scattering by the spark plasma during experiments was recorded by two methods.

In the first case, three photodiode were used. The distance from the first of them to the spark was constant (~ 25 cm) with an accuracy of ~ 1 mm and its displacement with respect to the laser beam axis could be varied from -50° to $+120^\circ$. The position of the second photodiode was fixed at an angle of $\sim 45^\circ$ to the beam axis. The solid angle of detection by these photodiodes of scattered laser radiation was determined by their apertures and was $\sim 10^{-4}$ sr. The third photodiode, which was used as a reference, controlled the amplitude and duration of a laser pulse in front of a focusing lens. The output signals of photodiodes were fed to the input of a Tektronix TDS5104B oscilloscope, which measured the amplitudes of pulses and delays between the maxima of pulses from the first and second photodiodes and also averaged these quantities and determined their dispersion. Radiation was attenuated with the help of calibrated NS and IKS optical filters mounted in front of all photodiodes.

The scattering diagrams measured by using vertically (the electric vector is perpendicular to the scanning plane of the first photodiode) and horizontally polarised laser pulses (a lens with the focal distance $f = 8$ mm was employed) are presented in Fig. 1. The scattering diagrams measured in the absence of the air breakdown are also shown in this figure. Points in the curves (*1*) and (*2*) are obtained by averaging over series of 20–30 measurements.

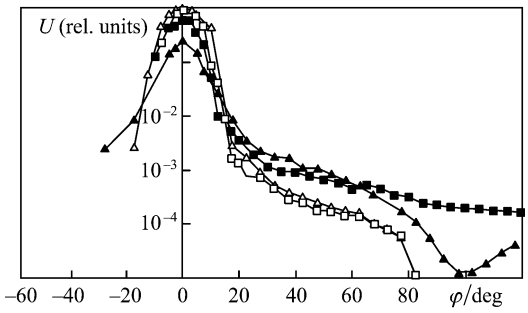

Figure 1. Laser radiation scattering diagrams for horizontally (▲, △) and vertically (■, □) polarised beams in the presence (dark points) and absence (light points) of the spark plasma. The radiation intensity is normalised to the maximum signal amplitude in the absence of the spark.

A reliable measurement of the relative delay between scattered radiation pulses detected by the first and second photodiodes proved to be possible only in the angular range $\varphi = 15^\circ - 80^\circ$, i.e. outside the initial laser beam cone. Figure 2 presents the results of two independent experiments. In the second experiment, the influence of radiation scattering by the surface and aperture of the lens with $f = 8$ mm was reduced by focusing 50-ns pulses through a diaphragm of diameter 600 μm in a 40-μm-thick foil.

The second measurement method proved to be more informative, and we used it to study in detail the diagram of laser radiation scattering by a plasma spark. The experimental scheme is presented in Fig. 3. In this case, a focon of diameter 40 mm was used whose output was in contact with a fibreoptic bundle. The second end of the bundle was made coincident with the entrance slit of a streak camera

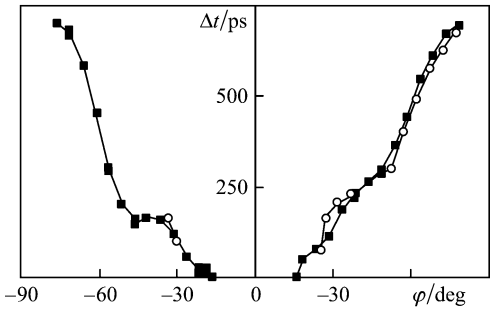

Figure 2. Delay of the laser pulse scattered by the spark plasma as a function of the observation angle.

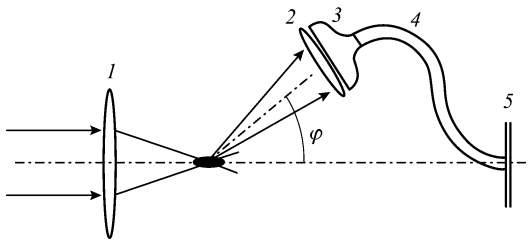

Figure 3. Scheme of spatiotemporal measurements of the diagram of laser radiation scattering by the spark plasma: (*1*) focusing lens; (*2*) field lens; (*3*) fibreoptic focon; (*4*) fibreoptic bundle; (*5*) streak-camera slit.

operating in the linear sweep regime. The orientation of the streak-camera slit corresponded to the focon rotation plane. By using this optical system, we investigated simultaneously the laser radiation scattering diagram in the angular range $\sim 15^\circ$ with a high time resolution. Because the reproducibility of the air breakdown by 3-ns pulses ($f = 20$ mm)

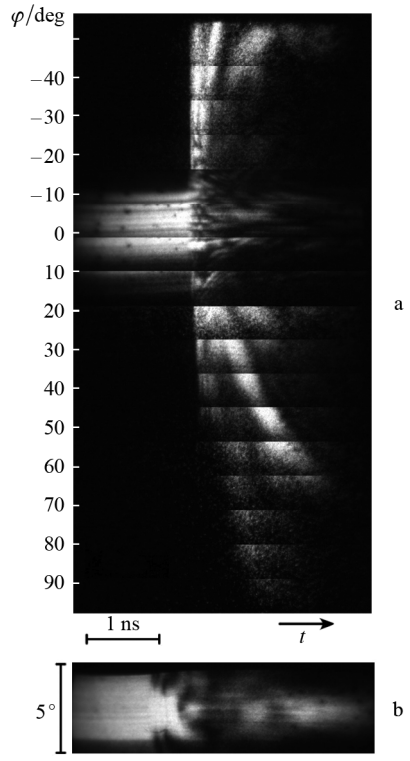

Figure 4. Spatiotemporal diagram of laser radiation scattering by the spark plasma (a) and its axial zone (b). The laser pulse duration is 3 ns.

was good enough, we could construct the general scattering diagram shown in Fig. 4a. By using the scheme in Fig. 3, we also obtained the scattering diagram for a lens with $f = 8$ mm and $\tau = 50$ ns.

The axial part of the laser beam transmitted through the spark plasma was observed with an angular resolution of $\sim 1^\circ$ by imagining it onto the streak-camera slit with the help of an objective. One can see from Fig. 4b that for $f = 20$ mm and 3-ns pulses, the laser radiation intensity exhibits a number of oscillations with characteristic times from 100 ps to 1 ns.

By using the streak camera, we also managed to detect the instant of the appearance of primary plasma during the air breakdown by laser radiation. The corresponding sweeps obtained for different focal distances of lenses and different laser pulse durations are presented in Fig. 5. Note that during pulse-integrated imaging of the laser-beam waist with a high spatial resolution (Fig. 6), as a rule, irrespective of the focal distance of lenses, laser pulse duration and the type of a focused radiation mode, the two scattering zones are located in the region near the focal plane of the lens. The distance between zones is 3–4 μm.

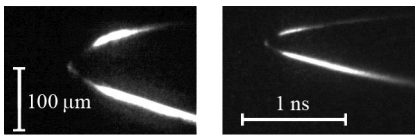

Figure 5. Spatiotemporal laser radiation scattering dynamics at the initial stage of the spark development during the air breakdown by 3-ns (a) and 50-ns (b) pulses at focal distances of lenses 20 mm (a) and 8 mm (b).

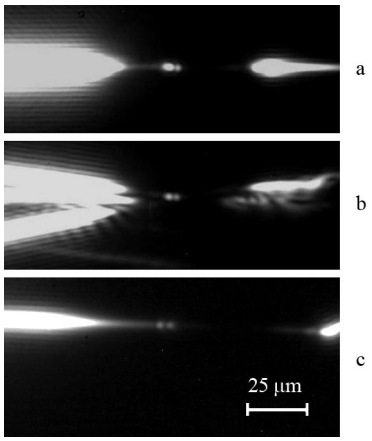

Figure 6. Images of the laser spark in the beam-waist region obtained by using focusing lenses with $f = 8$ mm (a, b) and 20 mm (c) and TEM_{00} (a, c) and TEM_{01} (b) radiation modes.

3. Discussion of the results

The diagram of laser radiation scattering by the spark plasma in air constructed based on oscilloscopic measurements for 50-ns pulses (Fig. 1) well coincides with diagrams obtained earlier experimentally and in model calculations for 1-ns pulses [9]. The dependence of the scattering intensity on the angle φ for horizontal and vertical polarisations is determined by the difference of the Fresnel reflection coefficients for laser radiation at the plasma boundary. The refection minimum for horizontal polarisation corresponds to $\varphi \sim 100^\circ$, which is close to $\varphi \sim 105^\circ$ obtained in [9] despite the difference in the pulse durations and focusing parameters ($2w/f \sim 0.06$ in [9] and ~ 0.4 in our case).

The scattered radiation pulse near the boundary of the laser-beam cone (Fig. 4a) and radiation propagated through the spark plasma (Fig. 4b) have the characteristic fine spatiotemporal structure, which is absent at large scattering angles (above 50°). The radiation intensity scattered in the angular range from 20° to 50° grows on for 50–60 ps (Fig. 4a). The total duration of the scattered radiation pulse during the air breakdown by 3-ns and 50-ns pulses is no more than 1–2 ns. The measured delay of the scattered pulse also lies in this range (Fig. 2). Note that the laser radiation scattering diagram presented in Fig. 4a is not quite symmetric with respect to the beam axis. Most likely this is explained by the sensitivity of the aspherical optics used in experiments to the laser-beam quality and focusing conditions (especially to the mutual mismatch of the lens and beam axes*).

Note first of all that the duration of a scattered radiation pulse is independent (or weakly depends) of the duration of a laser pulse producing a spark in air. This does not contradict the fact that upon imaging the reflection track from the side (at an angle of 90° to the laser-beam axis), the plasma front moving toward a lens is observed virtually during the entire laser pulse because the track image is formed by involving a set of angles, which is determined by the entire aperture of the microobjective (NA = 0.2–0.25). It follows from the diagram in Fig. 4a, sweeps of the spark image in Fig. 5 and dependences in Fig. 2, that side scattering appears with a delay with respect to the air breakdown instant. A low scattering intensity at the spark development stage (within 0.5–2 ns after the breakdown) also explains why model [9], in which the spark plasma was described by a sphere of radius 9.3 μm with the refractive index $n = 0.7 - 0.45i$, is consistent with experiments. The radius of a plasma sphere used in this model was averaged over the time interval corresponding to the expansion of the primary plasma up to the size of the order of the laser-beam waist in the lens focus.

In this case, if the plasma expansion rate is assumed equal to $10^6 - 10^7$ cm s^{-1}, then the interval 0.1–1 ns corresponds to the radius 9.3 μm. In this time interval, scattering from the spark plasma has the maximum intensity (Figs 4a and 5).

Near the boundaries of the laser-beam cone (Fig. 4) a quasi-periodic structure is observed, which is especially noticeable at angles 15°–30°. This structure and structure in Fig. 4b appear not due to scattering but due to the refraction and diffraction of laser radiation from the spark plasma. This is confirmed by the calculation, whose results are presented in Fig. 7. The plasma in the laser-beam waist was simulated in calculations by a circular phase screen of diameter increasing from 5 to 15 μm and by the phase varying linearly from $-\lambda$ to -2λ. The phase increment equal to one wavelength at a distance of 10 μm is appropriate to the electron concentration $n_e \sim 4 \times 10^{20}$ см$^{-3}$ ($n = 0.895$) corresponding to the complete ionisation of air.** Although the axial part of the time-dependent diffraction pattern in

* Aspherical lenses used in experiments are intended for operation in fibreoptic devices and are compensated only for spherical aberrations.

** The real part of the refractive index used in calculations [9] corresponds to the electron concentration that is twice as large as the electron concentration upon the complete ionisation of air.

Fig. 7a incompletely corresponds to the experiment, taking into account that absorption in the plasma, the real profile and dynamics of variation in the electron density is unknown, the results of the given calculation can be considered as quite consistent with experiments. Moreover, the calculation of the peripheral part of the diffraction pattern (Fig. 7b) also explains the quasi-periodic temporal structure of scattered laser radiation discovered earlier (see Fig. 1f from [12]).

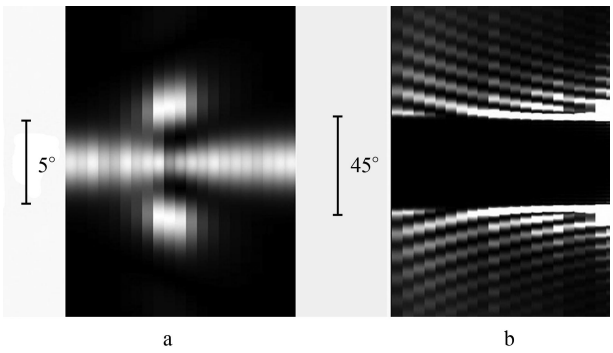

Figure 7. Axial (a) and peripheral (b) zone of laser beam diffraction from a circular phase screen with a linearly changing diameter (5 – 15 μm) and phase delay ($-\lambda \ldots -2\lambda$).

The spatiotemporal measurements of the expansion rate of the primary spark plasma in the waist region (Fig. 5) showed that at a distance of $\pm(20-25)$ μm from the focal plane this rate is only 2 – 3 times higher than the rate in the region of intense scattering of laser radiation. It is valid at least during the optical breakdown produced in air by 1.06-μm single-mode laser beams with the numerical aperture $2w/f \approx 0.4$. Taking into account the preceding, this confirms the assumptions made earlier [8] that the spark plasma in the nearest vicinity of the waist has a spherical shape with a centre in the focal plane of a focusing lens and reflection from the plasma boundary can occur only backward to the lens aperture. Thus, the theory of a point explosion can be applied to the first stage of the spark development of duration ~ 1 ns. In this case, the duration of the scattering pulse of the primary plasma (Fig. 5) is no more than 30 – 40 ps. Why the spatial structure of scattering from this plasma upon integral detection has the form of two points separated by a distance of $\sim 3-4$ μm along the optical axis is unclear.

4. Conclusions

The results of experiments with laser pulses of durations that differ by more than an order of magnitude have shown that laser radiation outside the laser beam cone is scattered mainly during the first one – two nanoseconds after the air break-down. At this stage of the optical breakdown development, the spark plasma is located in the vicinity of the laser-beam waist and has a nearly spherical shape. This is confirmed by our experimental results and calculations and their comparison with results reported in [9]. The scattering of laser radiation by the spark plasma observed at an angle of 90° occurs mainly at the later stages of the plasma existence, when the plasma size considerably exceeds the Rayleigh length of the focused laser beam and its shape differs from spherical. Some part of radiation outside the laser-beam cone is determined by diffraction from the spark plasma.

Acknowledgements. The authors thank R.V. Serov for useful discussions of the results of the paper.

References

1. Askar'yan G.A. *Zh. Eksp. Teor. Fiz.*, **42**, 1586 (1962).
2. Mayer G., Gires F. *Compt. Rend.*, **258**, 2039 (1964).
3. Garmire E., Chiao R., Townes C. *Phys. Rev. Lett.*, **16**, 347 (1966).
4. Brewer R.G., Lifsitz J.R. *Phys. Lett.*, **23**, 79 (1966).
5. Maker P.D., Terhune R.W., Savage C.M., in *Quantum Electronics III* (New York: Columbia Univer. Press, 1964) p.1559.
6. Alcock A.J., in *Laser Interaction and Related Plasma Phenomena* (New York: Plenum, 1972) Vol. 2, p.155.
7. Ostrovskaya G.V., Zaidel A.N. *Usp. Fiz. Nauk*, **111**, 579 (1973).
8. Malyutin A.A. *Kvantovaya Elektron.*, **38**, 462 (2008) [*Quantum Electron.*, **38**, 462 (2008)].
9. Wang Ch.C., Davis L.I. *Phys. Rev. Lett.*, **26**, 822 (1971).
10. Korobkin V.V., Alcock A.J. *Phys. Rev. Lett.*, **21**, 1433 (1968).
11. Belland P., De Michelis C., Mattioli M. *Opt. Commun.*, **4**, 50 (1971).
12. Glebov L.B., Efimov O.M., Petrovskii G.T., Rogovtsev P.N. *Kvantovaya Elektron.*, **12**, 2077 (1985) [*Sov. J. Quantum Electron.*, **15**, 1367 (1985)].
13. Bakos J., Földes I.B., Sörlei Zs. *J. Appl. Phys.*, **52**, 627 (1981).
14. Bufetov I.A., Bufetova G.A., Fedorov V.B. *Kvantovaya Elektron.*, **21**, 1177 (1994) [*Quantum Electron.*, **24**, 1092 (1994)].
15. Malyutin A.A., IlyukhinV.A. *Kvantovaya Elektron.*, **37**, 181 (2007) [*Quantum Electron.*, **37**, 181 (2007)].
16. Catalogue of ThorLabs Inc. (Newton, NJ, USA, 2007) Vol. 19.